MAGNETOHYDRODYNAMICS (MHD) CASSON FLUID FLOW OVER AN EXPONENTIAL STRETCHING SHEET

MOHAMMED I. B. S.[1], OLAYIWOLA R.O.[2], MOHAMMED A. A.[3] & NYOR N.[4]
[1]Department of Mathematics, Federal Polytechnic Bida, Nigeria.
[2,3,4]Department of Mathematics, Federal University of Technology Minna, Nigeria.
E-mail: babashabafu@gmail.com, olayiwolarasaq@yahoo.co.uk,
Phone: +234-806-548-7750

Abstract
This paper investigates MHD casson fluid flow over an exponentially stretching sheet. The governing partial differential equations were reduced to ordinary differential equations using similarity transformation. The reduced non-linear ordinary differential equations were solved analytically using iteration perturbation method and the results obtained were presented graphically. It was observed that casson, magnetic, unsteadiness, permeability and porosity parameters decrease the velocity profiles while ratio parameter, renold number, thermal and solutal grash of numbers enhance the velocity profiles. Also, magnetic parameter, radiative parameter, heat source, dufour number, chemical reaction and activation energy parameters enhance the temperature profile while prandtl number decreases the temperature profile. Soret number increase the concentration profile while chemical reaction parameter, activation energy parameter and schmidtl number decrease the concentration profile.

Keywords: Casson fluid, Dufour number, Iteration Perturbation Method, MHD, Non-Newtonian, Radiative Heat Flux, Soret number, Stretching sheet

Introduction
The study of real-life problems dealing with flow models of non-Newtonian fluids has received a special attention due to their several possible applications in engineering and industries. Due to the increasing significance of non – Newtonian fluids in industry, the stretching sheet concept has recently extended to fluids obeying non- Newtonian consecutive equation (Kumar & Gangadhar, 2015). Casson fluid is one type of non – Newtonian fluid, it can be defined as a shear thinning liquid which is supposed to have an infinite viscosity at zero rate of shear and a yield stress under which no flow occurs and zero viscosity at an infinite rate of shear (Sharada & Shnkar, 2016). Casson fluid is classified as a non-Newtonian fluid due to its rheological characteristics. These characteristics show shear stress-strain relationships that are significantly different from Newtonian fluid (Makanda *et al.* 2015). Viscosity is the quality that describes a fluid's resistance to flow. A fluid with high viscosity resists motion, while a fluid with low viscosity flows easily. More viscous substances, such as syrup and honey, take longer to pour than less viscous substances, such as water.

Asogwa and Ibe (2020) investigated MHD Casson fluid flow over a permeable stretching sheet with heat and mass transfer, the governing equations were transformed into self-similar nonlinear Ordinary differential equations and solved numerically using bvp4c MATLAB solver. The effect of the involved parameters on Velocity, Temperature, and Concentration, Skin friction coefficient, Nusselt number and Sherwood number were studied and numerical results were presented graphically and in tabular form. Saidulu and Lakshmi (2016) described the boundary layer flow of non-Newtonian Casson fluid accompanied by heat and mass transfer towards a porous exponentially stretching sheet with velocity slip and thermal slip conditions in presence of thermal radiation, suction/blowing, viscous dissipation, heat source/sink and

chemical reaction effects. They neglected the induced magnetic field since the magnetic Reynolds number for the flow was assumed to be very small. The governing equations were transformed into self-similar nonlinear Ordinary differential equations and solved numerically by an implicit finite difference scheme known as the Keller box method. Vedavathi *et al.* (2016) examined chemical reaction, radiation and dufour effects on Casson MHD fluid flow over a vertical plate with heat source/sink and the problem was solved numerically using perturbation technique. Wahiduzzaman *et al.* (2014) examined three-dimensional steady MHD casson fluid flow past a non-isothermal porous linearly stretching sheet, the governing equations were solved numerically using Nactsheim-swigert shooting iteration technique together with runge-kutta sixth order iteration.

The aim of this paper is to establish an analytical solution capable of predicting concentration, temperature and velocity distributions in a MHD casson fluid flow past a non-isothermal exponentially stretching sheet.

Model Formulation

Considering three dimensional (3D) transient incompressible flows past a non-isothermal exponentially stretching sheet. The sheet is stretched along the xy plane, while the fluid is placed along the z - axis; the uniform magnetic field is applied in z - direction that is perpendicular to the flow direction. Here, we assumed that the sheet was stretched with velocities $U_w = U_0 e^{\frac{x+y}{L}} (1-ct)^{-1}$ and $V_w = V_0 e^{\frac{x+y}{L}} (1-ct)^{-1}$ along the xy -plane respectively. A heat source/sink placed within the flow to allow for heat generation or absorption effects.

The rheological equation of state for an isotropic flow of casson fluid as stated by (Mohammed *et al.*, 2020) can be expressed as:

$$
\tau_{ij} = \begin{cases} 2\left(\mu_B + \dfrac{p_z}{\sqrt{2\pi}}\right)e_{ij}, \pi > \pi_c \\ \\ 2\left(\mu_B + \dfrac{p_z}{\sqrt{2\pi_c}}\right)e_{ij}, \pi < \pi_c \end{cases} \tag{1}
$$

In the above equation $\pi = e_{ij}e_{ij}$ and e_{ij} denotes the $(i,j)^{th}$ components of the deformation rate, π is the product of the deformation rate itself, π_c is the critical value of this product based on the non-Newtonian fluid model, μ_B is the plastic dynamic viscosity of the non-Newtonian fluid and p_z is the yield stress of the fluid. From (1), we obtain $\mu_B = \dfrac{1}{2}\dfrac{\tau_{ij}}{e_{ij}} - \dfrac{p_z}{\sqrt{2\pi}}$, $\upsilon = \dfrac{\mu_B}{\rho}$ and

$\beta = \dfrac{\sqrt{2\pi_c}}{p_z}\mu_B$

The boundary layer equations of three-dimensional incompressible casson fluids flow are given as follows

Continuity equation:

$$\frac{\partial u}{\partial x} + \frac{\partial v}{\partial y} + \frac{\partial w}{\partial z} = 0 \tag{2}$$

Momentum equations:

$$\left.\begin{array}{l} \dfrac{\partial u}{\partial t} + u\dfrac{\partial u}{\partial x} + v\dfrac{\partial u}{\partial y} + w\dfrac{\partial u}{\partial z} = \upsilon\left(1+\dfrac{1}{\beta}\right)\left[\dfrac{\partial^2 u}{\partial z^2}\right] - \dfrac{\sigma B^2}{\rho}u - \dfrac{\upsilon}{K}u - \Gamma u^2 + g_g \beta_T\left(T - T_\infty\right) \\[3mm] + g_g \beta_c\left(C - C_\infty\right) \end{array}\right\} \tag{3}$$

$$\frac{\partial v}{\partial t} + u\frac{\partial v}{\partial x} + v\frac{\partial v}{\partial y} + w\frac{\partial v}{\partial z} = \upsilon\left(1+\frac{1}{\beta}\right)\left[\frac{\partial^2 v}{\partial z^2}\right] - \frac{\sigma B^2}{\rho}v - \frac{\upsilon}{K}v - \Gamma v^2 \tag{4}$$

Energy equation:

$$\left.\begin{array}{l} \dfrac{\partial T}{\partial t} + u\dfrac{\partial T}{\partial x} + v\dfrac{\partial T}{\partial y} + w\dfrac{\partial T}{\partial z} = \dfrac{k_h}{\rho c_p}\left[\dfrac{\partial^2 T}{\partial z^2}\right] + \dfrac{D_m k_T}{T_m c_S}\dfrac{\partial^2 C}{\partial z^2} + \dfrac{\sigma B^2}{\rho}\left(u^2 + v^2\right) + \\[3mm] \dfrac{Q_1}{\rho c_p}\left(T - T_\infty\right) - \dfrac{1}{\rho c_p}\dfrac{\partial q_r}{\partial z} + \beta_{EE}k_r^2\left(T - T_\infty\right)^n.\left(C - C_\infty\right)e^{-\frac{E_a}{k(T - T_\infty)}} \end{array}\right\} \tag{5}$$

Species equation:

$$\frac{\partial C}{\partial t} + u\frac{\partial C}{\partial x} + v\frac{\partial C}{\partial y} + w\frac{\partial C}{\partial z} = D_m\frac{\partial^2 C}{\partial z^2} + \frac{D_m k_T}{T_m}\frac{\partial^2 T}{\partial z^2} - k_r^2\left(T - T_\infty\right)^n.\left(C - C_\infty\right)e^{-\frac{E_a}{k(T - T_\infty)}} \tag{6}$$

Subject to the initial and boundary conditions:

$$\left.\begin{array}{l} u(z,t) = 0, v(z,t) = 0, w = 0, T(z,t) = T_\infty, C(z,t) = C_\infty \ \ for\, t = 0\ for\ all\ \ z \\[2mm] u = U_w, v = V_w, T = T_w, C = C_w\ at\ \ z = 0 \\[2mm] u \to 0, v \to 0, T \to T_\infty, C \to C_\infty\ \ at\ \ z \to \infty \end{array}\right\} \tag{7}$$

Where , u , v and w are the velocity component in the direction of x, y and z respectively, β is the casson fluid parameter, υ is the kinematic viscosity, B is the magnetic induction, B_0 is constant, K and Γ are permeability and the inertia coefficient of porous medium, T is temperature, C is the concentration of the fluid, β_T and β_C are the coefficient of volume expansion for temperature and concentration differences respectively, β_{C_0} and β_{T_0} are constants, Q_1 is heat source, Q_0 is constant, k_T is the thermal diffusivity ratio, α_h is the thermal diffusivity, δ is the density of the fluid, g_g is acceleration due to gravity, σ is the electrical conductivity, k_h is the thermal conductivity, c_p is the specific heat capacity at constant pressure, c_S is the concentration susceptibility, T_∞ is the free stream temperature, T_m is the mean fluid temperature, D_m is the coefficient of mass diffusivity, k_r is the chemical reaction rate, k_{r_0} is constant, $\beta_{EE}(=\pm 1)$ is the exothermic/endothermic parameter,

$(T - T_\infty)^n.(C - C_\infty)e^{-\frac{E_a}{k(T-T_\infty)}}$ is the Arrhenius function where n is the dimensionless exponent fitted rate constant typically lie in the range $-1 < n < 1$, E_a is the activation energy, k is the Boltzmann constant k_0 is constant and the radiative heat flux q_r is described by Roseland approximation such that $q_r = -\dfrac{4\sigma_1}{3k_1}\dfrac{\partial(T^4)}{\partial z}$ where σ_1 and k_1 are the Stefan Boltzmann constant and mean absorption coefficient respectively. We Assume that the differences in temperature within the flow is such that T^4 can be expressed as a linear combination of the temperature, we expand T^4 in a Taylor series about T_∞.

Method of Solution

We now introduce the similarity variables as:

$$
\left.
\begin{aligned}
&\eta = \sqrt{\frac{U_0}{2\upsilon L(1-ct)}}\, e^{\frac{x+y}{2L}} z, \quad u = \frac{U_0}{(1-ct)} e^{\frac{x+y}{L}} f'(\eta), \quad v = \frac{U_0}{(1-ct)} e^{\frac{x+y}{L}} g'(\eta), \\[2mm]
&T = T_\infty + \frac{T_0}{(1-ct)} e^{\frac{x+y}{L}} \theta(\eta), \quad C = C_\infty + \frac{C_0}{(1-ct)} e^{\frac{x+y}{L}} \phi(\eta), \\[2mm]
&w = -\sqrt{\frac{\upsilon U_0}{2L(1-ct)}}\, e^{\frac{x+y}{2L}} \left(f + \eta f' + g + \eta g'\right) \\[2mm]
&k_r = \frac{k_{r0}}{(1-ct)^{\frac{1}{2}}} e^{\frac{x+y}{2L}}, \quad K = \frac{(1-ct)}{K_0 e^{\frac{x+y}{L}}}, \quad B = \frac{B_0}{(1-ct)^{\frac{1}{2}}} e^{\frac{x+y}{2L}} \\[2mm]
&k = \frac{k_0(1-ct)}{e^{\frac{x+y}{L}}}, \quad Q_1 = \frac{Q_0}{(1-ct)} e^{\frac{x+y}{L}}, \quad \beta_T = \frac{\beta_{T_0}}{(1-ct)} e^{\frac{x+y}{L}}, \quad \beta_C = \frac{\beta_{C_0}}{(1-ct)} e^{\frac{x+y}{L}}
\end{aligned}
\right\}
\tag{9}
$$

The transformed equations with the boundary conditions are:

$$
\left(1 + \frac{1}{\beta}\right) f''' + (f + \eta f' + g + \eta g') f'' - 2(f' + g')\left(f' + \frac{\eta}{2} f''\right) - (M + K_p) f' - \Lambda f'^2
$$
$$
- \frac{a}{R_e}\left(f' + \frac{\eta}{2} f''\right) + G_{r_\theta} \theta + G_{r_\phi} \phi = 0
\tag{10}
$$

$$
\left(1 + \frac{1}{\beta}\right) g''' + (f + \eta f' + g + \eta g') g'' - \frac{a}{R_e}\left(g' + \frac{\eta}{2} g''\right) - 2(f' + g')\left(g' + \frac{\eta}{2} g''\right)
$$
$$
- (M + K_p) g' - \Lambda g'^2 = 0
\tag{11}
$$

$$\frac{1}{P_r}\theta''(\eta)+\frac{R}{P_r}\theta''(\eta)+(f+\eta f'+g+\eta g')\theta'(\eta)-2(f'(\eta)+g'(\eta))\left(\theta(\eta)+\frac{\eta}{2}\theta'(\eta)\right)+$$

$$M\left(f'^2(\eta)+g'^2(\eta)\right)-\frac{a}{R_e}\left(\theta(\eta)+\frac{\eta}{2}\theta'(\eta)\right)+Q_h\theta(\eta)+\delta\phi(\eta)e^{-\frac{\varepsilon}{\theta}}+D_u\phi''(\eta)=0 \tag{12}$$

$$\frac{1}{P_r}\theta''(\eta)+\frac{R}{P_r}\theta''(\eta)+(f+\eta f'+g+\eta g')\theta'(\eta)-2(f'(\eta)+g'(\eta))\left(\theta(\eta)+\frac{\eta}{2}\theta'(\eta)\right)+$$

$$M\left(f'^2(\eta)+g'^2(\eta)\right)-\frac{a}{R_e}\left(\theta(\eta)+\frac{\eta}{2}\theta'(\eta)\right)+Q_h\theta(\eta)+\delta\phi(\eta)e^{-\frac{\varepsilon}{\theta}}+D_u\phi''(\eta)=0 \tag{13}$$

$$\left.\begin{array}{l}f(0)=0, \qquad g(0)=0,\ f'(0)=1, \qquad g'(0)=\alpha, \quad \theta(0)=1, \qquad \phi(0)=1\\ f'\to 0\ as\ \eta\to\infty,\ g'\to 0\ as\ \eta\to\infty,\ \theta\to 0\ as\ \eta\to\infty,\ \phi\to 0\ as\ \eta\to\infty\end{array}\right\} \tag{14}$$

Where

$$G_{r_\theta}=\frac{2Lg\beta_{T_0}T_0}{U_0^2},G_{r_\phi}=\frac{2Lg\beta_{C_0}C_0}{U_0^2},\frac{a}{R_e}=\frac{2Lc}{U_0e^{\frac{(x+y)}{L}}},M=\frac{2L\sigma B_0^2}{\rho U_0},\alpha_h=\frac{k_h}{\rho c_p},$$

$$K_p=\frac{2L\upsilon K_0}{U_0},\Lambda=2L\Gamma,S_r=\frac{D_mk_T}{T_m}\frac{C_0}{\upsilon T_0},\frac{1}{S_c}=\frac{D_m}{\upsilon},\delta=\frac{2L\beta_{EE}k_{r_0}^2C_0}{T_0U_0}$$

$$,Q_h=\frac{2LQ_0}{\rho c_p U_0},R=\frac{16T_\infty^3\sigma_1}{3k_1k_h},\frac{1}{P_r}=\frac{k_h}{\rho c_p\upsilon},D_u=\frac{D_mk_T}{T_mc_S}\frac{C_0}{\upsilon T_0},\alpha=\frac{V_0}{U_0}$$

Now, we begin with the initial approximate solution (Olayiwola, 2016; Mohammed *et al.*, 2020):

$$\left.\begin{array}{l}f_0=\frac{1}{b}\left(1-e^{-b\eta}\right)\\[2mm]g_0=\frac{\alpha}{b}\left(1-e^{-b\eta}\right)\end{array}\right\} \tag{15}$$

Substituting (15) into (10) to (13) and expressing the solutions in the form:

$$\begin{array}{l}f(\eta)=f_0(\eta)+pf_1(\eta)+...\\ g(\eta)=g_0(\eta)+pg_1(\eta)+...\\ \theta(\eta)=\theta_0(\eta)+p\theta_1(\eta)+...\\ \phi(\eta)=\phi_0(\eta)+p\phi_1(\eta)+...\end{array} \tag{16}$$

We obtain,

$$
\left.
\begin{aligned}
f(\eta) &= \frac{1}{q_2}\left(1 - e^{-q_2\eta}\right) + p\left(\begin{array}{l} d_1\eta e^{-q_2\eta} - d_2\eta^2 e^{-q_2\eta} + d_3 e^{-q_2\eta} - d_4 e^{-q_6\eta} - d_5 e^{-2q_2\eta} - d_6 e^{-q_3\eta} \\ -d_7 e^{-bS_r\eta} + q_{16} \end{array}\right) \\[2mm]
g(\eta) &= \frac{\alpha}{q_2}\left(1 - e^{-q_2\eta}\right) + p\left(q_{21}\eta e^{-q_2\eta} + q_{22} e^{-q_2\eta} - q_{23}\eta^2 e^{-q_2\eta} - q_{25} e^{-2q_2\eta} + \frac{q_{26}}{q_2^2} e^{-q_2\eta} + q_{27}\right) \\[2mm]
\theta(\eta) &= e^{-q_3\eta} + p\left(\begin{array}{l} q_{35}\eta^2 e^{-q_3\eta} + q_{36}\eta e^{-q_3\eta} + q_{37} e^{-q_3\eta} + q_{38} e^{-q_6\eta} - q_{39} e^{-q_{32}\eta} + q_{40} e^{-2q_2\eta} \\ + q_{41} e^{-bS_c\eta} + q_{42} e^{q_{34}\eta} - \frac{q_{43}}{q_3} e^{-q_3\eta} \end{array}\right) \\[2mm]
\phi(\eta) &= e^{-bSc\eta} + p\left(\begin{array}{l} q_{44}\eta^2 e^{-bS_c\eta} + q_{45}\eta e^{-bS_c\eta} - q_{46} e^{-bS_c\eta} - q_{47} e^{-q_{52}\eta} + q_{48} e^{-q_{53}\eta} - q_{49} e^{q_{54}\eta} \\ + q_{50} e^{-2q_3\eta} - \frac{q_{51}}{bS_c} e^{-bS_c\eta} \end{array}\right)
\end{aligned}
\right\}
\tag{17}
$$

Where,

$$q_{18} = \left(\frac{q_2\alpha}{b} + \alpha^2\frac{q_2}{b}\right), \quad q_{20} = 2\alpha + 2\alpha^2 + \Lambda\alpha^2, \quad q_{21} = \frac{q_{17}}{q_2^2 b_1} - 2\frac{q_{82}}{q_2^3 b_1}, \quad q_{22} = 2\frac{q_{17}}{q_2^3 b_1} - \frac{q_{18}}{b_1 q_6^2(q_2 - q_6)} - 3\frac{q_{82}}{q_2^4 b_1}, q_{23} = \frac{q_{82}}{2q_2^2 b_1},$$

$$q_{26} = \left(\frac{q_{18}}{b_1 q_6(q_2 - q_6)} - \frac{q_{17}}{q_2^2 b_1} + \frac{q_{82}}{q_2^3 b_1} + \frac{q_{20}}{2q_2 b_1}\right)q_2, \quad q_{27} = q_{25} - q_{22} - \frac{q_{26}}{q_2^2}, \quad q_{28} = b_3 - Q_h + \frac{q_3}{b} - bq_3 + \frac{\alpha q_3}{b}, \quad q_{29} = \frac{b_3 q_3}{2},$$

$$q_{30} = \left(\frac{q_3}{b} + \frac{\alpha q_3}{b}\right), \quad q_{31} = 2 + 2\alpha, \quad q_{32} = q_2 + q_3, \quad q_{33} = M(1 + \alpha^2), \quad q_{34} = q_3 - bS_c, \, q_3 = \frac{b}{b_5}, q_{35} = \frac{q_{29}}{2q_3 b_5},$$

$$q_{36} = \left(\frac{q_{29}}{q_3^2 b_5} - \frac{q_{28}}{q_3 b_5}\right), q_{37} = \left(\frac{q_{29}}{q_3^3 b_5} - \frac{q_{28}}{q_3^2 b_5}\right), q_{38} = \frac{q_{30}}{q_6 b_5(q_3 - q_6)}, q_{39} = \frac{q_{31}}{q_{32} b_5(q_3 - q_{32})}, \quad q_{40} = \frac{q_{33}}{2q_2 b_5(q_3 - 2q_2)}, \quad q_{25} = \frac{q_{20}}{4q_2 b_1},$$

$$q_{41} = \left(\frac{\delta}{bS_c b_5(q_3 - bS_c)} + \frac{D_u(bS_c)^2}{bS_c b_5(q_3 - bS_c)}\right), q_{42} = \frac{\delta\varepsilon}{q_{34} b_5(q_3 + q_{34})}, q_{43} = (q_{37} + q_{38} - q_{39} + q_{40} + q_{41} + q_{42})q_3,$$

$$q_2 = \frac{b}{b_1}, \quad q_3 = \frac{b}{b_5}, \quad b_5 = \frac{1 + R}{p_r}, q_4 = b_3 + \frac{q_2}{b} + \alpha\frac{q_2}{b} - bq_2 + b_2, \quad q_5 = \left(\frac{q_2}{b} + \alpha\frac{q_2}{b}\right), \quad q_6 = b + q_2,$$

$$q_7 = 2 + 2\alpha + \Lambda, \quad q_8 = \frac{b_3 q_2}{2}, q_9 = \frac{q_4}{b_1}, \quad q_{10} = \frac{q_5}{b_1(q_2 - q_6)}, \quad q_{11} = \frac{q_7}{b_1 q_2}, \quad q_{12} = \frac{q_8}{2b_1}, \quad q_{13} = \frac{G_{r_\theta}}{b_1(q_2 - q_3)},$$

$$q_{14} = \frac{G_{r_\phi}}{b_1(q_2 - bS_c)}, \quad d_1 = \frac{q_9}{q_2^2} - 3\frac{q_{12}}{q_2^3}, \quad d_2 = \frac{q_{12}}{q_2^2}, \quad d_3 = 2\frac{q_9}{q_2^3} - 4\frac{q_{12}}{q_2^4} + \frac{q_{15}}{q_2^2}, \quad d_4 = \frac{q_{10}}{q_6^2},$$

$$d_5 = \frac{q_{11}}{4q_2^2}, \quad d_6 = \frac{q_{13}}{q_3^2}, \quad d_7 = \frac{q_{14}}{(bS_c)^2}, \quad q_{82} = \frac{b_3 q_2}{2}\alpha, \quad q_{17} = b_3\alpha + b_2\alpha + \frac{q_2\alpha}{b} + \alpha^2\frac{q_2}{b} - bq_2\alpha,$$

$$q_{42} = \frac{\delta\varepsilon}{q_{34} b_5(q_3 + q_{34})}, q_{43} = (q_{37} + q_{38} - q_{39} + q_{40} + q_{41} + q_{42})q_3,$$

$$, \quad q_{28} = b_3 - Q_h + \frac{q_3}{b} - bq_3 + \frac{\alpha q_3}{b}, \quad q_{29} = \frac{b_3 q_3}{2}, \quad q_{30} = \left(\frac{q_3}{b} + \frac{\alpha q_3}{b}\right), \quad q_{31} = 2 + 2\alpha, \quad q_{32} = q_2 + q_3, q_{33} = M(1 + \alpha^2),$$

$$q_{34} = q_3 - bS_c, \, q_3 = \frac{b}{b_5}, q_{35} = \frac{q_{29}}{2q_3 b_5}, \quad q_{36} = \left(\frac{q_{29}}{q_3^2 b_5} - \frac{q_{28}}{q_3 b_5}\right), q_{37} = \left(\frac{q_{29}}{q_3^3 b_5} - \frac{q_{28}}{q_3^2 b_5}\right), q_{38} = \frac{q_{30}}{q_6 b_5(q_3 - q_6)},$$

$$q_{39} = \frac{q_{31}}{q_{32}b_5(q_3 - q_{32})}, \quad q_{40} = \frac{q_{33}}{2q_2 b_5(q_3 - 2q_2)}, \quad q_{41} = \left(\frac{\delta}{bS_c b_5(q_3 - bS_c)} + \frac{D_u(bS_c)^2}{bS_c b_5(q_3 - bS_c)}\right), q_{42} = \frac{\delta\varepsilon}{q_{34}b_5(q_3 + q_{34})},$$

$$q_{43} = (q_{37} + q_{38} - q_{39} + q_{40} + q_{41} + q_{42} - 1)q_3, \quad q_{44} = \frac{b_3 b(S_c)^2}{bS_c 4}, q_{45} = \left(\frac{b_3 b(S_c)^2}{2(bS_c)^2} - \frac{1}{b}\left(\begin{array}{c}b_3 + \delta + S_c \\ + \alpha S_c - b^2 S_c\end{array}\right)\right),$$

$$q_{46} = \left(\frac{1}{b^2 S_c}(b_3 + \delta + S_c + \alpha S_c - b^2 S_c) - \frac{b_3 b(S_c)^2}{2(bS_c)^3}\right), \quad q_{47} = \frac{S_c}{b(b + bS_c)}(S_c + \alpha S_c), \quad q_{48} = \frac{S_c(2 + 2\alpha)}{q_2(q_2 + bS_c)}q_{49} = \frac{\varepsilon\delta S_c}{q_3(q_3 - bS_c)},$$

$$q_{50} = \frac{S_r S_c q_3^2}{2q_3(bS_c - 2q_3)}, \quad q_{51} = (q_{50} - q_{46} - q_{47} + q_{48} - q_{49} - 1)bS_c, \quad q_{52} = b + bS_c, \quad q_{53} = (q_2 + bS_c), \quad q_{54} = (q_3 - bS_c)$$

Results and Discussion

The governing partial differential equations were reduced to ordinary differential equations using similarity transformation and the reduced non-linear ordinary differential equations were solved using iteration perturbation method. The computations were done for the values of

$\beta = 0.2$, $R = 0.1$, $P_r = 0.71$, $R_e = 0.1$, $S_c = 0.22$, $S_r = 0.2$, $D_u = 0.5$, $G_{r\theta} = 0.1$, $G_{r\phi} = 0.1$, $\alpha = 1$, $K_p = 0.4$, $a = 1$, $\Lambda = 0.5$, $\delta = 0.5$, $\varepsilon = 0.01$, $p = 0.01$, $b = 2.3062$ $Q_h = 0.2$ and $M = 0.5$ except otherwise as shown in figures (1 - 26) below.
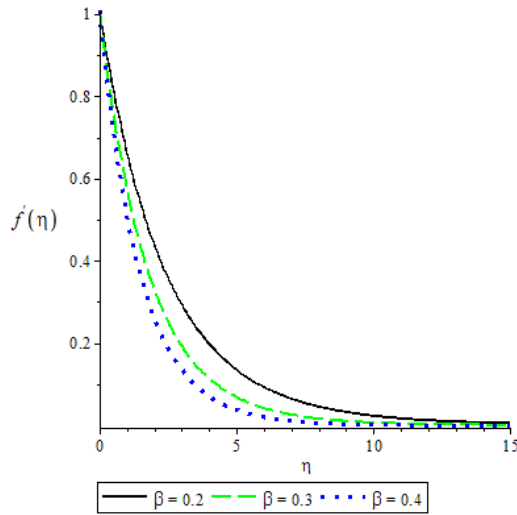
Figure 1: Effect of β on Velocity Profile $f'(\eta)$
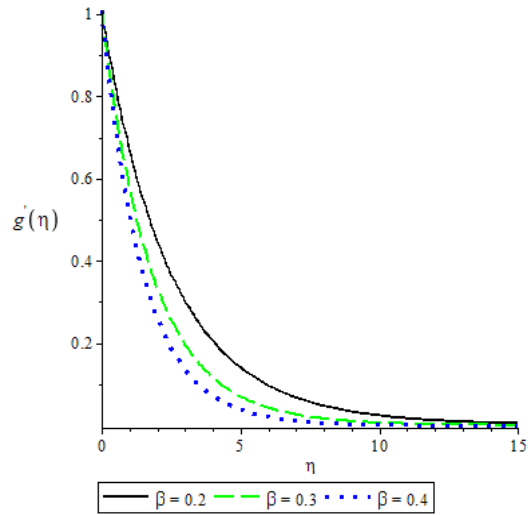
Figure 2: Effect of β on Velocity Profile $g'(\eta)$
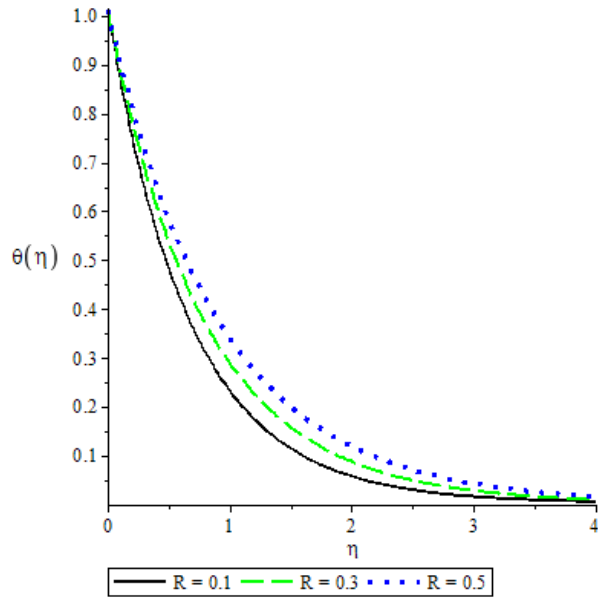
Figure 3: Effect of R on Temperature Profile
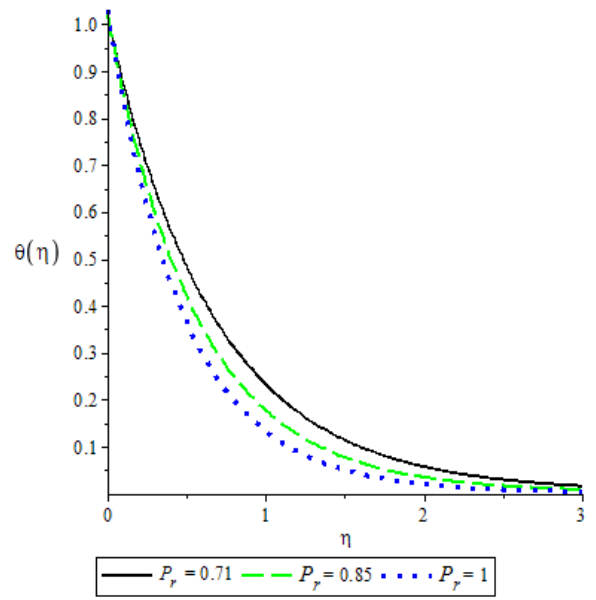
Figure 4: Effect of P_r on Temperature Profile
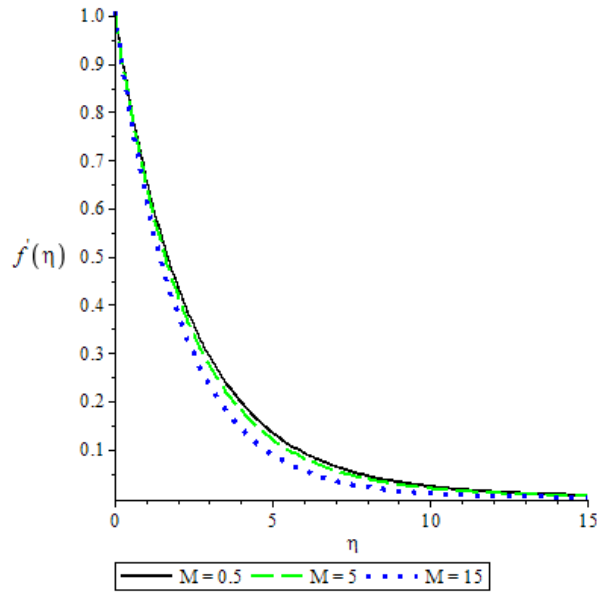
Figure 5: Effect of M on Velocity Profile $f'(\eta)$
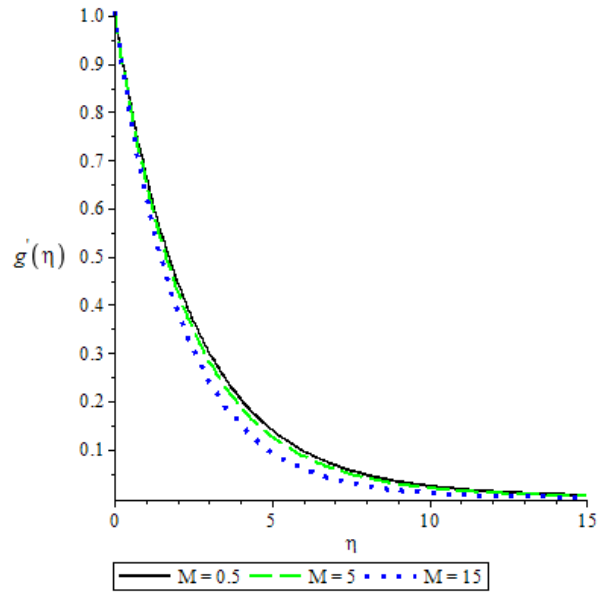
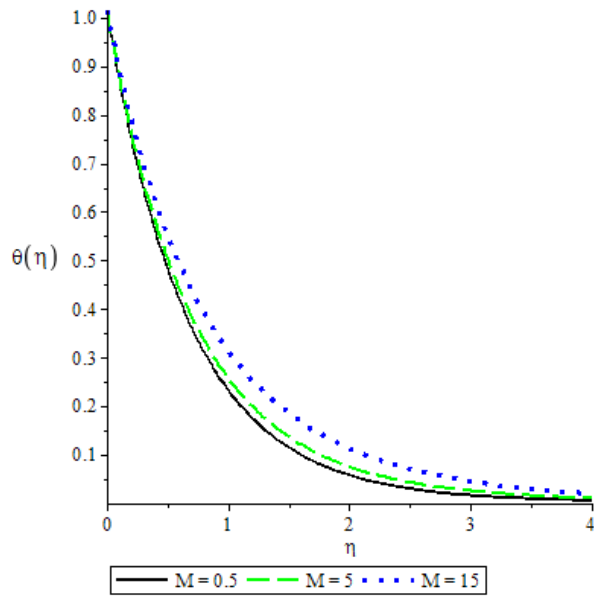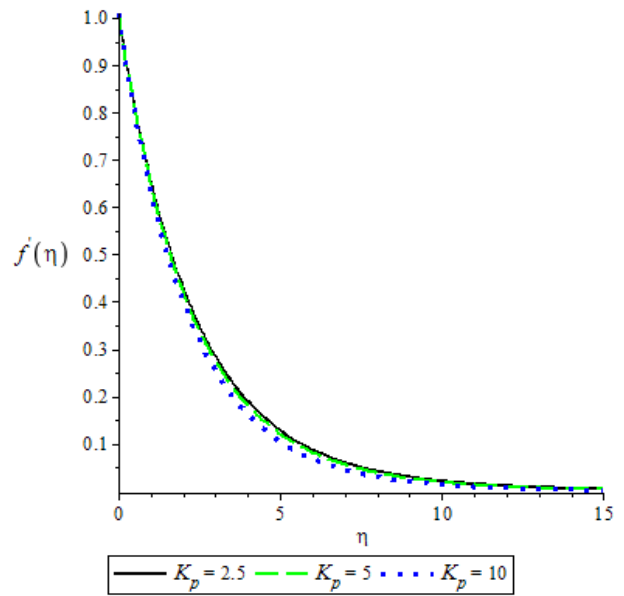
Figure 6: Effect of M on Velocity Profile $g'(\eta)$

Figure 7: Effect of M **on Temperature Profile** $\theta(\eta)$

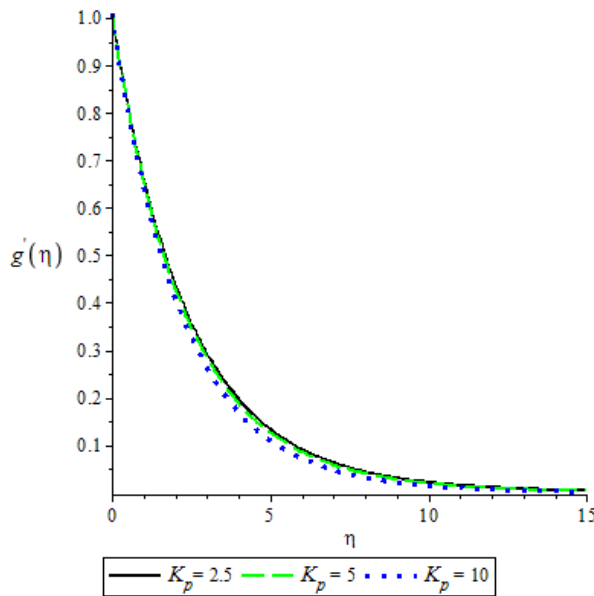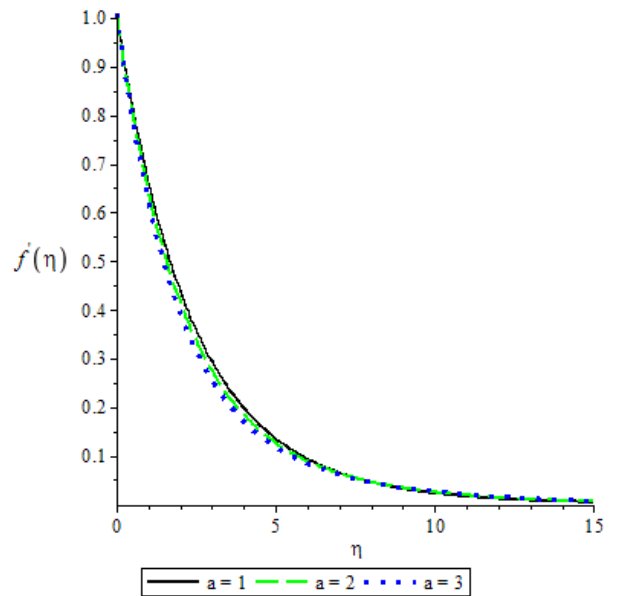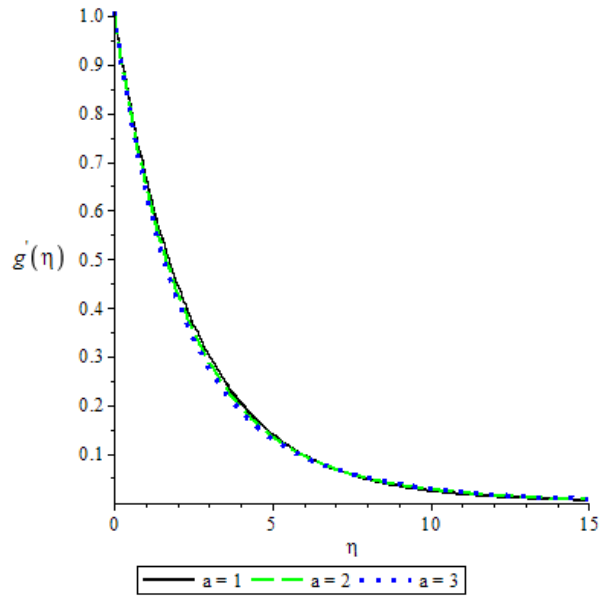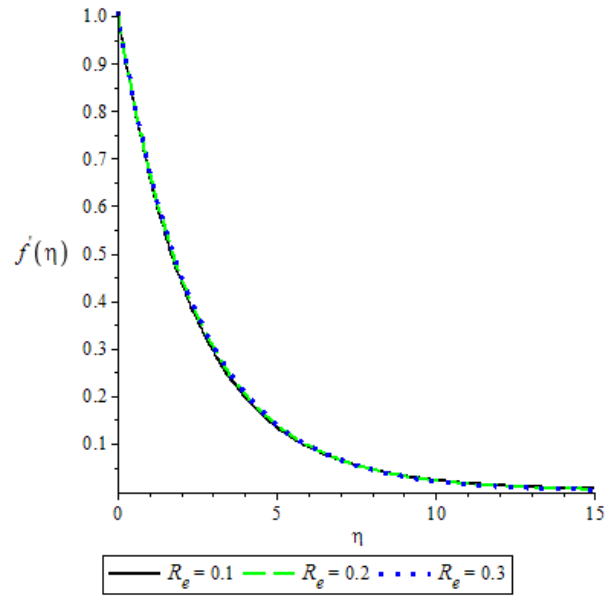**Figure 8: Effect of** K_p **on Velocity Profile** $f'(\eta)$

Figure 9: Effect of K_p **on Velocity Profile** $g'(\eta)$

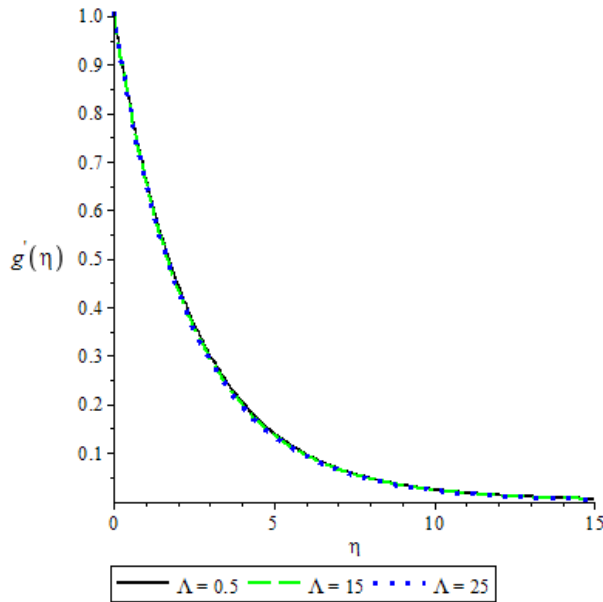**Figure 10: Effect of** a **on Velocity Profile** $f'(\eta)$

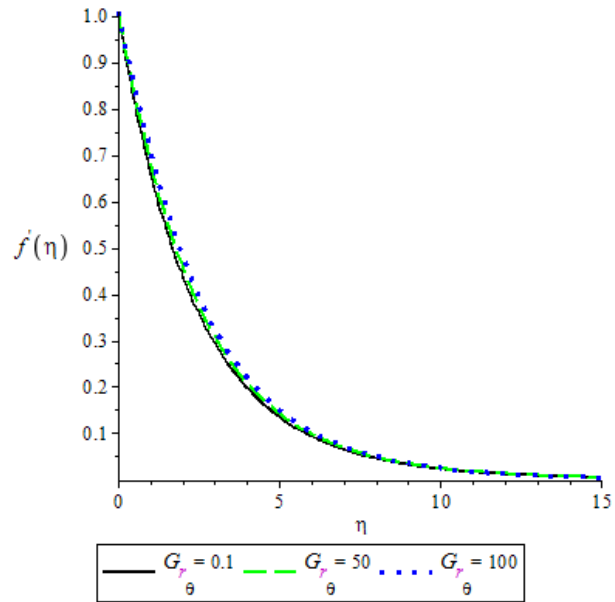**Figure 11: Effect of a on Velocity Profile $g'(\eta)$**

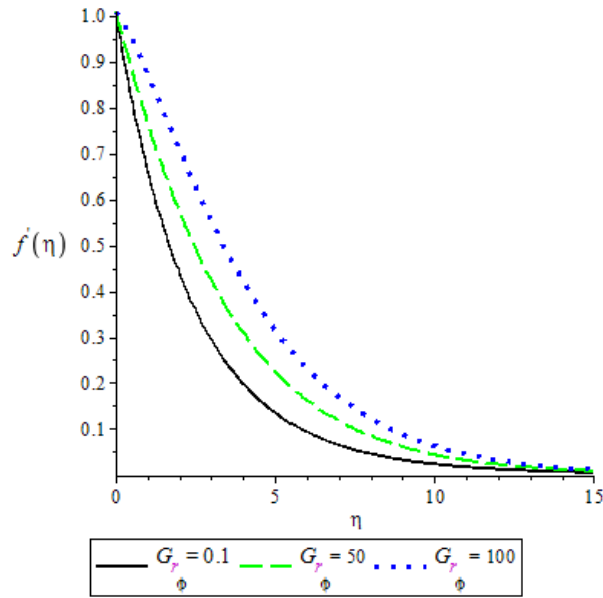**Figure 12: Effect of R_e on Velocity Profile $f'(\eta)$**
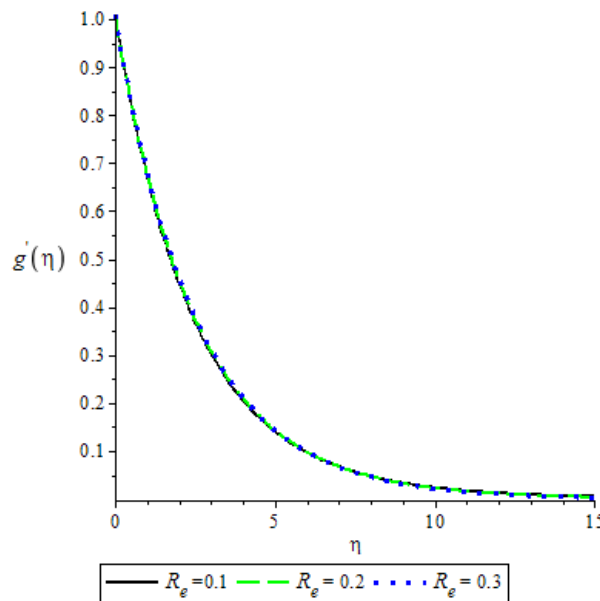
Figure 13: Effect of R_e on Velocity Profile $g'(\eta)$
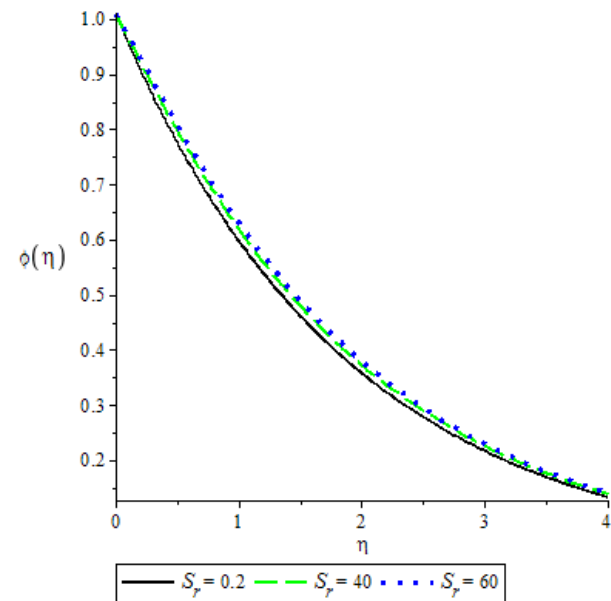
Figure 14: Effect of S_r on Concentration Profile $\phi(\eta)$
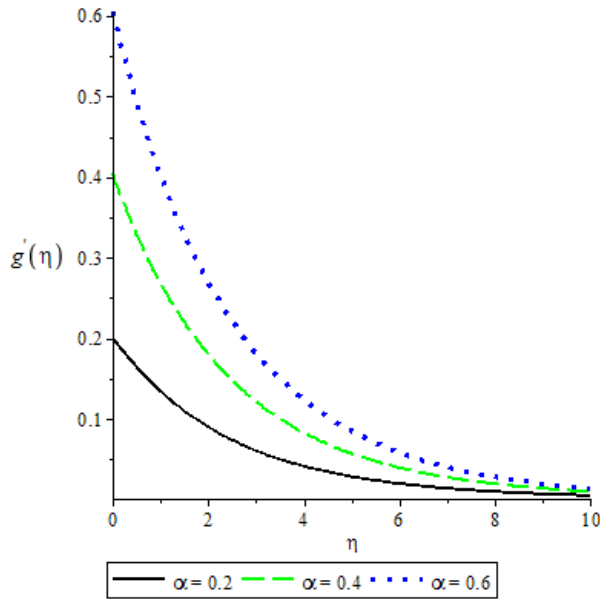
Figure 15: Effect of α on Velocity Profile $g'(\eta)$
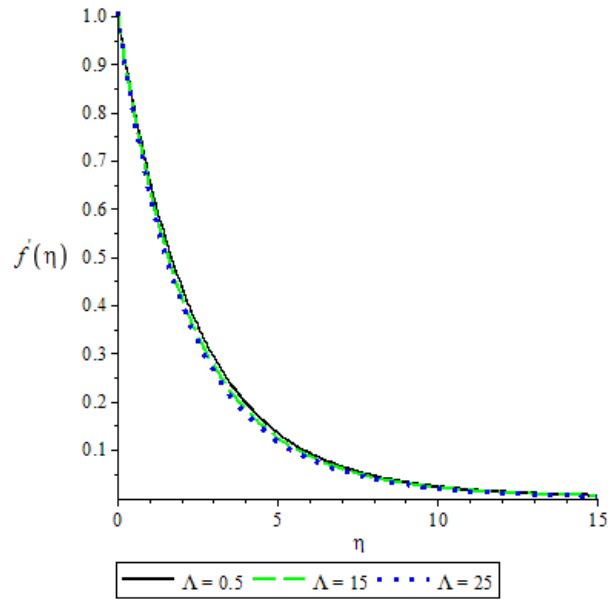
Figure 16: Effect of Λ on Velocity Profile $f'(\eta)$

Figure 17: Effect of Λ on Velocity Profile $g'(\eta)$

Figure 18: Effect of G_{r_θ} on Velocity Profile $f'(\eta)$

Figure 19: Effect of G_{r_ϕ} on Velocity Profile $f'(\eta)$
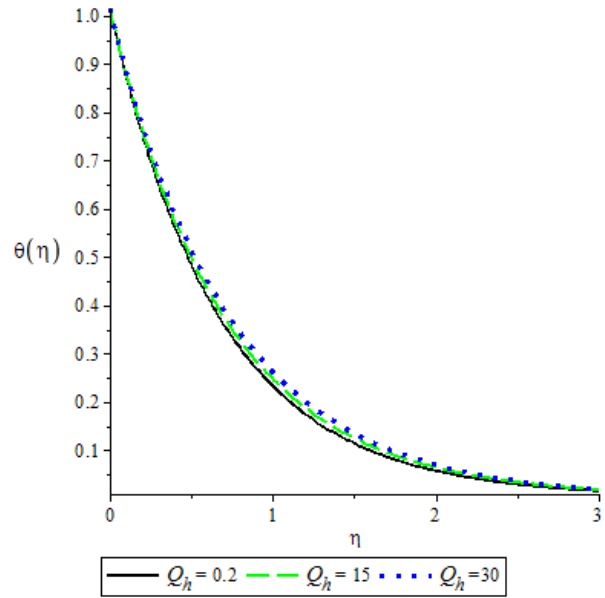

Figure 20: Effect of Q_h on Temperature Profile $\theta(\eta)$
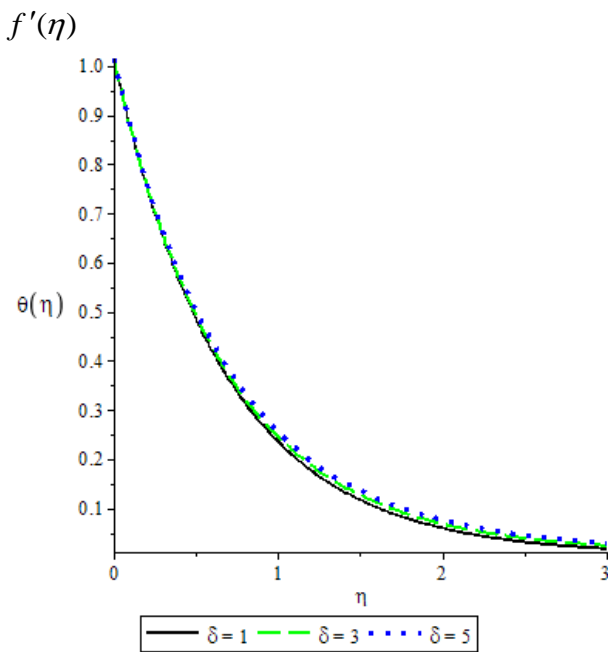
Figure 21: Effect of δ on Temperature Profile $\theta(\eta)$

Figure 22: Effect of δ on Concentration Profile $\phi(\eta)$
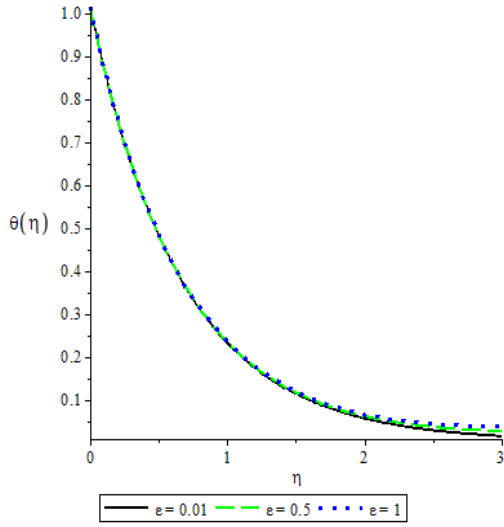
Figure 23: Effect of ε on Temperature Profile $\theta(\eta)$

Figure 24: Effect of ε on Concentration Profile $\phi(\eta)$
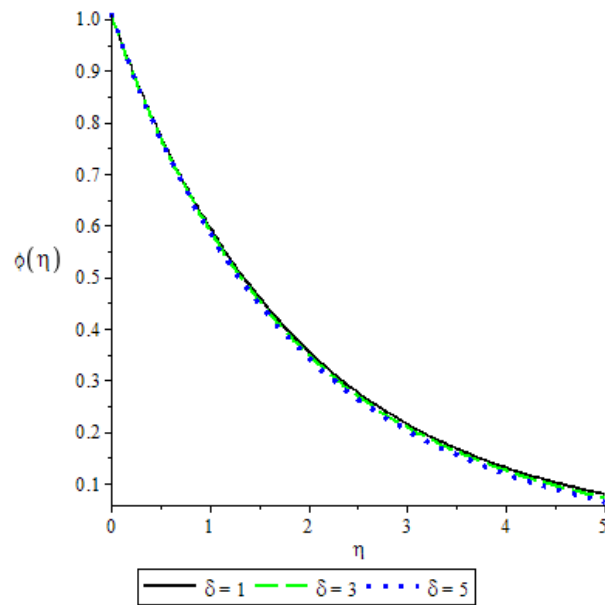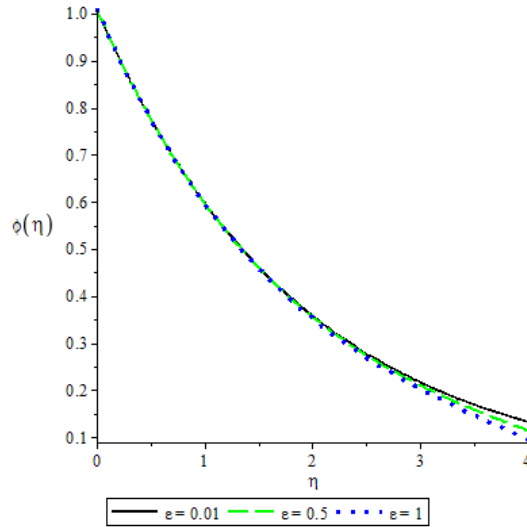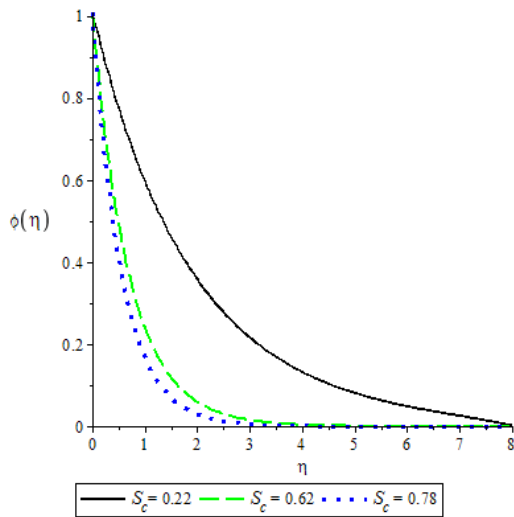

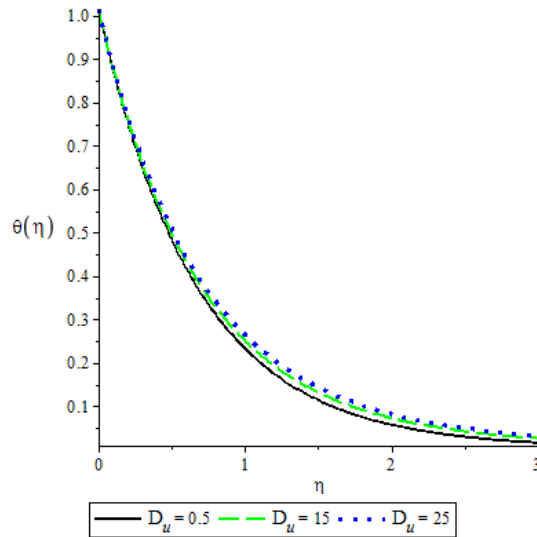**Figure 25: Effect of S_c on Concentration Profile $\phi(\eta)$**

Figure 26: Effect of D_u on Temperature Profile $\theta(\eta)$

Figures 1 and 2 show the velocity profiles against the similarity variable η for different values of casson parameter. It was observed from these figures that as casson parameter increases, the fluid velocity distribution decreases inside the boundary layer. Figure 3 and 4 depicts the effects of radiation parameter and prandtl number on the temperature profile. It was observed that increase in radiation parameter increases the temperature profile while increase in prandtl number decreases the temperature profile. In figures 5 to 7, it was observed that increase in magnetic parameter decreases the velocity profiles and enhance the temperature profile. From figures 8 to 11, we observed that increase in permeability and unsteadiness parameters lead to decrease in velocity profiles. Figure 12 to 14 shows that as local renold number R_e increases,

the velocity profiles increases while soret number S_r enhances the concentration profile as depicted in figure 14. Figures 15 to 19, shows that increase in ratio parameter increase the velocity profile, increase in porosity parameter decrease the velocity profiles and increase in thermal and solutal grashof numbers enhances the velocity profile due to thermal and solutal buoyancy effects. From figures 20 to 26 it was observed that increase in heat source parameter, dufour number, chemical reaction and activation energy parameters enhance the temperature profile while the concentration profile decreases with increase in chemical reaction parameter, activation energy parameter and schmidtl number.

Conclusion
Based on the above results it was observed that:
   i. Casson, magnetic, unsteadiness, permeability and porosity parameters decrease the velocity profiles respectively
   ii. Local Reynold number, ratio parameter, thermal and solutal grashof numbers enhance the velocity profiles
   iii. Magnetic parameter, radiative parameter, heat source, dufour number, chemical reaction and activation energy parameters enhance the temperature profile
   iv. Prandtl number decreases the temperature profile
   v. Soret number increases the concentration profile
   vi. Chemical reaction parameter, activation energy parameter and schmidtl number decrease the concentration profile

References

Asogwa, K. K., & Ibe, A. A. (2020). A study of MHD casson fluid over a permeable stretching sheet with heat and mass transfer. *Journal of Engineering Research and Report (JERR), 16(2), ISSN: 2582-2926,* 10-25.

Kumar, S., & Gangadhar, P. K. (2015). Effects of chemical reaction on slip flow of MHD casson fluid over a stretching sheet with heat mass transfer. *Advances in Applied Science Research,* 6(8), 205-223.

Kumar, S., Prasanna, T., & Gangadhar, K. (2015). Moment and thermal slip flow of MHD casson fluid over a stretching sheet with viscous dissipation, *International Journal of Modern Engineering Research (IJMER), 5(5), ISBN 2249-6645.*

Makanda, G., Shaw, S., & Sibanda, P. (2015). Diffusion of chemically reactive species in casson fluid flow over an unsteady stretching surface in porous medium in the presence of a magnetic field. *Mathematical Problems in Engineering,* Article ID 724596.

Mohammed, I. B. S., Saidu, Y. V., Olayiwola, R. O., & Abubakar, A. D. (2020). Magnetohydrodynamic casson fluid flow over an exponential stretching sheet with effect of radiation. *International Journal of Pure and Applied Science (IJPAS),* 12(9), 66-80.

Olayiwola, R. O. (2016). Modeling and analytical simulation of a laminar premixed flame impinging on a normal solid surface. *Nigerian Journal of Mathematics and Applications (NJMA)*, 25, 226 – 240.

Saidulu, N., & Lakshmi, A. V. (2016). Slip effects on MHD flow of casson fluid over an exponentially stretching sheet in presence of thermal radiation, heat. Source/Sink and Chemical Reaction. *International Journal of Advanced in Engineering and Technology*, 3(1), 47-55.

Sharada, K., & Shankar, B. (2016). Three-dimensional MHD mixed convection casson fluid flow over an exponential stretching sheet with the effect of heat generation. *British Journal of Mathematics and Computer Science*, 19(6), 1-8.

Vedavathi, N., Dharmaiah, G., Balamurugan, K. S., & Kumar, C. G. (2016). Chemical reaction radiation and dufour effects on casson magneto hydro dynamics fluid flow over a vertical plate with heat. Source/Sink. *Global Journal of Pure and Applied Mathematics*, 12(1), 191-200.